Chytrid fungi construct actin-rich pseudopods, implicating actin regulators WASP and SCAR in an ancient mode of cell motility

Authors: Lillian K. Fritz-Laylin,[a] Samuel J. Lord,[a] and R. Dyche Mullins[a,1]

[a] Department of Cellular and Molecular Pharmacology, Howard Hughes Medical Institute, University of California, San Francisco CA 94158, USA.

[1] Corresponding author:
Department of Cellular and Molecular Pharmacology
University of California, San Francisco
Genentech Hall, Room N312, Box 2200
600 16th Street
San Francisco, CA 94158
Phone number: 415-502-4838
Email: dyche@mullinslab.ucsf.edu

Abstract

Various cells scattered throughout the eukaryotic tree crawl across surfaces or through three-dimensional environments. Evidence now indicates that cell crawling is not a single behavior, but rather a collection of processes, driven by different molecular mechanisms. Understanding these mechanisms and their evolutionary relationships first requires narrowly defining mechanical modes of locomotion, and then identifying phenotypic and molecular markers of each. Here, we focus on a widely dispersed form of cell crawling characterized by dynamic, actin-filled pseudopods and weak, nonspecific adhesion to external substrates, a mode we refer to as "*α*-motility." Finding *α*-motility in cells ranging from free-living amoebae to immune cells hints at a single evolutionary origin of this complex process. By mining recently published genomic data, we identified a clear trend: only organisms with both WASP and SCAR/WAVE—two activators of branched actin assembly—make dynamic, three-dimensional pseudopods. While SCAR has been shown in some organisms to be an important driver of pseudopod formation, a role for WASP in this process is less clear. We hypothesize that these genes together represent a genetic signature of *α*-motility, and both proteins are used for pseudopod formation. We test our hypothesis by depleting WASP from human neutrophils, and confirm that both proteins are needed for explosive actin polymerization, pseudopod formation, and rapid cell migration. We also found that WASP and SCAR colocalize to the same dynamic signaling structures in living cells. Moreover, genomic retention of WASP together with SCAR also correctly predicts the presence of pseudopods in the disease-causing fungus *Batrachochytrium dendrobatidis*, making it the first fungus reported to undergo *α*-motility. By narrowing our focus to a single mode of cell migration while expanding our phylogenetic analysis to a variety of eukaryotes, we identified WASP together with SCAR as a conserved genetic marker of fast, low-adhesion cell crawling. Our cell-biology experiments argue that this conservation reflects their collaboration in the explosive actin assembly required to build dynamic pseudopods. These results represent the clearest evidence for a widely distributed mode of cell crawling with a single evolutionary origin.

Introduction

Eukaryotic cells move using several distinct modes of locomotion, including crawling and flagella-driven swimming. The stereotyped architecture of flagella and the conservation of their protein components render the evolutionary history of cell swimming relatively transparent. In contrast, “crawling motility” is a collection of processes whose functional and evolutionary relationships are not well understood [1-3]. Some crawling cells require dedicated adhesion molecules to make specific, high-affinity contacts with their surroundings, while other cells rely on weaker, nonspecific interactions. Crawling cells also employ different mechanisms to advance their leading edge, either assembling polymerized actin networks to push the plasma membrane forward, or detaching the membrane from the underlying cytoskeleton to form a rapidly expanding bleb. Furthermore, some cell types have been shown to use contractile forces to generate forward movement [4-6]. Different cells can also employ different sets of molecules to drive similar modes of crawling. In an extreme example, nematode sperm have evolved a method of crawling in which polymer assembly advances the leading-edge membrane but, in these cells, the force-generating polymer networks are composed of “major sperm protein” rather than actin. Given this variety of crawling behaviors, it is clear that one cannot simply assume that the underlying molecular mechanisms are the same.

The best understood mode of crawling is the slow (1-10 μm/hour) creeping of adherent animal cells, including fibroblasts and epithelial cells [7]. These cells move by extending sheet-like protrusions called lamellipodia while gripping substrate molecules using integrins, often clustered into large focal adhesions. Although clinically and physiologically important, this form of adhesion-based crawling is unique to the animal lineage, and largely restricted to molecular “highways” formed by the extracellular matrix. In contrast, many motile cells—including free-living amoebae and human immune cells—make three-dimensional, actin-filled pseudopods and navigate complex environments at speeds up to 20 μm/min (100-1000× faster than creeping fibroblasts) without forming specific molecular adhesions [8,9]. Although this mode of fast cell crawling has been called “amoeboid motility,” this term is also used to describe a range of behaviors, including cell motility that relies on membrane blebs rather than actin-filled pseudopods [2]. To narrow our mechanistic focus we use the term “*α*-motility” specifically to describe cell crawling that is characterized by: (i) highly dynamic three-dimensional, actin-filled pseudopods at the leading edge; (ii) fast migration, often on the order of 10 μm/min; and (iii) the absence of specific, high-affinity adhesions to the extracellular environment. Some organisms using *α*-motility may also employ additional methods of generating forward movement, such as contractility or retrograde flow [4-6], but here we focus on a phenotype that is readily observable in diverse species, including non-model organisms.

Organisms with cells capable of this form of locomotion appear throughout the eukaryotic tree, and we hypothesize that *α*-motility reflects a single, discrete process that arose early in eukaryotic evolution and has since been conserved. If this hypothesis is correct, then elements of this ancient process—specific molecules and mechanisms—should be conserved and still associated with cell crawling in distantly

related organisms that employ *α*-motility. Such molecular remnants would help to unravel the evolutionary history of cell locomotion, and might enable us to predict the existence of specific modes of motility in unexplored species. Identifying genes associated with a process such as *α*-motility is not trivial because the core machinery driving pseudopod formation (e.g. actin and the Arp2/3 complex) is shared with other cellular activities, including some types of endocytosis [10]. We therefore turned our attention to upstream regulators of actin assembly. WASP and SCAR (also known as WAVE) are widely conserved "nucleation promoting factors" that stimulate branched actin network assembly by the Arp2/3 complex in response to various upstream cellular signals [11-13] and promote different levels of Arp2/3 activity [14]. The broad phylogenetic distributions of WASP and SCAR gene families suggest that both genes are ancient and likely to have been present in the eukaryotic ancestor [15,16], making them appealing candidates for genetic markers of *α*-motility.

SCAR plays a major role in the formation of lamellipodia required for slow, adhesion-dependent migration of fibroblasts [17,18] as well as pseudopods at the leading edge of fast-moving amoebae and neutrophils [19,20]. In contrast, the involvement of WASP genes (including mammalian WASP and N-WASP) in cell crawling is less clear. Several studies argue that WASP family proteins do not participate in membrane protrusion or cell migration [21-23], while other studies suggest a direct role for WASP in pseudopod formation and/or cell crawling [24-29]. Part of this confusion may reflect differences in regulation and assembly of substrate-attached lamellipodia by slow-moving cells and three-dimensional pseudopods made by fast-moving cells. Here, we clarify the role of WASP in cell migration by focusing specifically on the regulation of actin assembly in pseudopods used for *α*-motility.

To understand the regulation of the actin cytoskeleton during pseudopod formation, we exploited the diversity of organisms that use *α*-motility. By comparing the genomes of many eukaryotes, we found that only organisms with genes encoding *both* WASP and SCAR make pseudopods. We validated this molecular signature using a positive test (a new prediction of *α*-motility in a little-studied organism) as well as a negative test (depleting the protein disrupts pseudopod formation in well-studied cells). Differentiating *α*-motility from slow/adhesive cell migration helps clarify much of the confusion over WASP's importance in cell motility, and shifts the major question from whether WASP *or* SCAR is required for motility in a given single cell type, to how WASP and SCAR work *together* to construct and maintain pseudopods in many species. The retention of WASP and SCAR by organisms that form pseudopods represents the first molecular support, to our knowledge, for a single origin of this widespread form of cell motility.

Results

Evolutionary retention of both WASP and SCAR/WAVE correlates with pseudopod formation

To trace the evolutionary history of *α*-motility, we first determined which sequenced eukaryotic organisms might employ *α*-motility, combing the literature for references to organisms with cells that form pseudopods. Eukaryotic phyla fall into at least six large

clades, and species with sequenced genomes and that form pseudopods can be found in most (**Fig 1** and **Table S1**).

On to this map of the phylogenetic distribution of pseudopods, we overlayed the conservation of WASP and SCAR/WAVE genes, using a recently published, manually curated database of nucleation promoting factors from genomes spanning eukaryotic diversity [16]. Multiple analyses indicate that both WASP and SCAR were present in the last common ancestor of eukaryotes [15,16], and therefore argue that a lack of either gene reflects loss during evolution.

To understand whether these gene loss events reveal a significant pattern, we compared the conservation of individual nucleation promoting factors across large evolutionary distances with the ability to assemble pseudopods. We observed a nearly perfect correlation between the conservation of WASP and SCAR and pseudopod formation (**Fig 1**); the only exceptions from this correlation were two little-studied species of chytrid fungi.

For example, *no* plant cells build pseudopods and *no* sequenced plant genomes contain a WASP ortholog. Similarly, multicellular fungi—the dikarya—lack SCAR and are also not known to build pseudopods. Conversely, *almost* all sequenced genomes of Amoebozoan species (including dictyostelids) encode orthologs of WASP and SCAR, and *almost* all move with the help dynamic, actin-rich pseudopods. A revealing example is the amoeba *Entamoeba histolytica*, which does not form actin-filled psuedopods but instead moves using blebs [30], and also lacks genes encoding both WASP and SCAR. We were unable to find a single example of an organism lacking either WASP or SCAR that is capable of constructing motile, actin-rich pseudopods. We did, however, find two little-studied species of chytrid fungi that had retained both nucleation promoting factors, but are not known for *α*-motility, *Allomyces macrogynus* and *Batrachochytrium dendrobatidis.*

We took a two-pronged approach to testing our hypothesis that retention of WASP together with SCAR serves as a molecular signature of pseudopod formation. First, we took the more traditional approach and confirmed that both genes are involved in pseudopod formation in mammalian cells. We followed this with an evolution-based approach by verifying the ability of this molecular signature to predict the capacity for pseudopod formation in chytrid fungi.

WASP and SCAR localize to the same dynamic arcs within pseudopods of human neutrophils

Our evolutionary evidence indicates that WASP and SCAR may *both* be required to build pseudopods. To test this hypothesis directly, we turned to human cell lines capable of forming pseudopods. HL-60 cells are derived from an acute myeloid leukemia [31] and retain many features of hematopoietic cells, including expression of hematopoietic WASP and the capacity to differentiate into fast-migrating neutrophils with dynamic pseudopods [32].

Using immunofluorescence microscopy, we found that WASP concentrates in two distinct locations within migrating HL-60 cells: punctate foci distributed throughout the cell and a broad zone near the leading edge (**Fig S1A**). To follow the dynamics of WASP localization in live cells, we created an HL-60 line stably expressing full-length WASP fused at the N-terminus to the red florescent protein TagRFP-T. By confocal fluorescence microscopy, the TagRFP-WASP localization pattern was similar to that of endogenous WASP as determined by immunofluorescence (**Fig S1B**).

Others have shown that the SCAR regulatory complex localizes to fast-moving, anterograde **"**waves" that break against the leading edge of actively migrating HL-60 cells [33]. This localization pattern is most easily observed using total internal reflection fluorescence (TIRF) microscopy, which illuminates a ~100 nm thick region of the cell near the ventral surface [34]. Using TIRF microscopy on rapidly migrating HL-60 cells, we observed that TagRFP-WASP concentrates near the leading edge in linear arcs that move in an anterograde direction, similar to previously observed patterns of the SCAR regulatory complex [33].

To see whether WASP and the SCAR travel together in the same waves, we introduced TagRFP-WASP into cells expressing YFP-Hem1, a core component of the SCAR regulatory complex [33]. TIRF microscopy of these cells revealed that WASP and the SCAR regulatory complex move together in the same dynamic, linear arcs (**Fig 2** and **Movie S1**). Interestingly, however, the localization patterns of the two are not identical: the SCAR complex generally appears in continuous arcs, while WASP forms a more punctate approximation of the SCAR pattern. Within the resolution limits of our imaging, the localization patterns move together, with neither protein consistently leading the other. This dynamic localization pattern suggests that both WASP and SCAR activate the Arp2/3 complex in leading-edge pseudopods, promoting assembly of the branched actin networks required for membrane protrusion.

WASP participates in pseudopod assembly and locomotion of neutrophils

To investigate whether WASP is involved in pseudopod assembly, we generated anti-WASP small hairpin RNAs (shRNAs), expression of which results in a >90% reduction of WASP protein by HL-60 cells (**Fig 3A**). We next examined whether WASP-depleted (WASP-KD) cells can form pseudopods. In a gradient of chemoattractant (the peptide fMet-Leu-Phe), wildtype HL-60 cells become strongly polarized with broad, actin-rich pseudopods used to rapidly move toward the source of chemoattractant (**Fig 3** and **Movie S2**). Compared to control, 50% fewer WASP-KD cells formed pseudopods (**Fig 3E**). Despite numerous attempts, we never succeeded in developing WASP-KD cell lines in which this phenotype was 100% penetrant. Although this might reflect the function of residual WASP protein, it is also consistent with the fact that WASP knockout mice show only a partial defect in neutrophil migration *in vivo* [35].

In addition to the defect in pseudopod formation, approximately 30% of WASP-KD cells form large protrusions that taper to a point, reminiscent of a rhinoceros horn (**Fig 3C,D**, **Fig S2**, and **Movie S2** WASP-KD cells 11, 32, 33, 39 and 42, for example). To verify its specificity, we rescued this "rhino" phenotype by expressing a functional WASP

containing three silent mutations in the sequence targeted by to the shRNA (**Fig 3F**). Additionally, a control shRNA that targets a separate region of the WASP gene results in a significantly smaller rescue effect on both WASP expression and the number of cells with the rhino phenotype (**Fig 3A,F**). Immunofluorescence combined with phalloidin staining of polymerized actin revealed that the aberrant rhino protrusions contain actin filaments but lack microtubules (**Fig 3D**). The expression of a probe specific for polymerized actin (mCherry fused to calponin homology domain of Utrophin, Utr261 [36]) revealed a highly dynamic and, surprisingly, hollow actin filament network inside the protrusions (**Fig S2**). This distribution—enriched near the membrane but depleted from the core of the protrusion—is more reminiscent of cortical actin networks than of filopodia, which are packed tight with actin bundles [37].

To determine the effect of WASP depletion on cell locomotion, we imaged cells migrating through a chemoattractant gradient in a 5 μm tall glass chamber [38]. Tracking individual cells revealed a severe migration defect in WASP-KD cells: while control cells move at an average speed of 2.2 μm/min, cells with rhino protrusions are almost completely immotile (**Fig 3G** and **Movies S2**). We conclude that HL-60 cells use WASP, along with SCAR [20], for normal pseudopod formation and efficient *α*-motility.

The human WASP paralog, N-WASP, is thought to contribute to endocytosis in mammalian cells [39,40], and its yeast ortholog is required for endocytosis [41]. We, therefore, tested the effect of WASP depletion on endocytosis. Pseudopod formation involves drastic transmogrification of the cytoskeleton, and inhibits endocytosis in wildtype cells. Therefore, due to their differing capacities for pseudopod formation, no useful comparisons can be made of endocytosis of differentiated control and WASP-KD cells. Instead, we quantified actin-mediated endocytosis by measuring the uptake of a pulse of fluorescent transferrin by undifferentiated cell populations that do not form pseudopods [42]. The resulting time course revealed no statistically significant difference in actin-mediated endocytosis or vesicular recycling in WASP-KD cells compared to control cells (**Fig S3**), arguing that the defects in *α*-motility are not due to gross defects in endocytosis.

WASP-depleted neutrophils polymerize less actin in response to chemoattractant

Addition of chemoattractant to non-polar (quiescent) HL-60 cells induces a burst of actin polymerization that drives polarization and pseudopod formation, nearly doubling the cell's filamentous actin content within 30 seconds of stimulation. This response is already known to depend on the activity of the SCAR regulatory complex [20]. To determine what role WASP might play in this explosive actin assembly, we synchronized pseudopod formation by stimulating populations of quiescent HL-60s with fMLP, fixed and stained the cells with phalloidin at different time points, and analyzed total polymerized actin content in each cell by fluorescence-activated cell sorting (FACS, **Fig 3B**). In the absence of chemoattractant, the amount of filamentous actin in quiescent WASP-KD cells is roughly equal to that in control cells. However, as reported for SCAR-depleted cells [20], WASP-KD cells have greatly reduced actin polymerization (**Fig 3B**) at both short (30 seconds) and long times (3 minutes) following stimulation. This reduced actin polymerization indicates that WASP, like SCAR, is central to the

explosive actin polymerization required for cell polarization and subsequent pseudopod formation.

WASP and SCAR genes predict *α*-motility in chytrid fungi

The only potential exceptions to the tight correlation between actin-rich pseudopods and the genomic retention of WASP and SCAR were two deeply branching species of fungi, the chytrids *Allomyces macrogynus* and *Batrachochytrium dendrobatidis* (*Bd*). These chytrid species contain genes encoding both WASP and SCAR, but have not been reported in the literature to migrate using pseudopods. We were, however, able to find references to pseudopod formation by unsequenced infectious species related to *A. macrogynus* (*Catenaria anguillulae*), which may employ these structures for motility across the surface of its target host [43,44]. However, because chytrid fungi are not a monophyletic group, but rather comprise multiple deeply branching clades, one cannot assume that more distant species share this capacity. Therefore, we used *Bd* as a predictive test of our hypothesis that WASP and SCAR genes represent a marker for *α*-motility.

Like other species of chytrid fungi, the lifecycle of *Bd* has two stages: a large (10-40 μm) reproductive zoosporangium, which releases a host of small (3-5 μm), motile, flagellated zoospores [45,46]. These infectious zoospores can form cysts beneath the skin of an amphibian host that develop into new zoosporangia to complete the life cycle [46]. We searched for *α*-motility in *Bd* zoospores because, unlike the sessile cyst and zoosporangium, these free-swimming flagellates lack a cell wall and have been reported to assume non-uniform shapes with dense “cytoplasmic extensions” [45].

To restrict the fast-swimming *Bd* zoospores to the imaging plane, we confined cells between a glass coverslip and slide, held apart by glass microspheres. In initial experiments, we observed only a small fraction (<1%) of zoospores forming pseudopod-like protrusions. The rarity of pseudopod-forming cells suggested that *α*-motility might only occur during a short phase of the life cycle. We therefore enriched for cells of the same age by washing zoosporangia to remove previously released zoospores and collecting flagellates released during the subsequent two hours.

During the first 6 hours after release from the zoosporangium, 30-50% of zoospores create dynamic pseudopod-like protrusions (**Fig 4** and **Movie S3**) that extend from the cell body at a rate of 25 +/- 9 μm/min, consistent with speeds expected for pseudopods [47,48]. Unlike blebs, these cellular protrusions are not spherical but irregularly shaped and amorphous—similar to the actin-rich pseudopods of amoebae and neutrophils. We found that pseudopod-forming *Bd* cells do not adhere strongly to glass surfaces (even when coated with fibronectin, concalavin-A, or collagen) and require micron-scale confinement for motility.

Some pseudopod-forming zoospores retained flagella, while other cells had clearly lost or resorbed their flagella and strongly resembled free-living amoebae (**Fig 4B** and **Movie S3**). We also observed cells switching from crawling to flagellar motility and vice versa, as well as cells rapidly retracting their flagella into the cell body (**Movie S4**). To

ensure that these crawling cells were not contaminating organisms, we obtained independently isolated *Bd* cultures from three different laboratories, and observed the same type of *α*-motility in each.

Chytrid pseudopods contain actin and require Arp2/3 activity

Using our assay to image chytrid zoospores, we next investigated whether extension of *Bd* pseudopods is driven by assembly of branched actin networks, as in other cells crawling using *α*-motility. We first fixed the cells to preserve the actin cytoskeleton and then stained them with fluorescent phalloidin to reveal a thin shell of cortical actin surrounding the cell body and a dense network of filamentous actin filling the pseudopod (**Fig 4E**). To determine whether assembly of the pseudopodial actin network requires the nucleation and branching activity of the Arp2/3 complex, we incubated zoospores with CK-666, a small molecule that inhibits actin nucleation by mammalian and fungal Arp2/3 complexes [49]. Addition of 10 μM of CK-666 reduced the number of cells with active protrusions by almost half (**Fig 4C**), and this effect could be reversed by washing out the drug (**Fig 4D** and **Table S2**). These experiments reveal that protrusion of *Bd* pseudopods requires Arp2/3-dependent actin assembly.

Discussion

Our results reveal that, across eukaryotic phyla, cells capable of constructing actin-rich pseudopods and performing fast, low-adhesion crawling retain, in addition to the Arp2/3 complex, two distinct activators of its actin nucleation activity: WASP and SCAR/WAVE. Organisms without the capacity to crawl in this manner turn out to have lost one or both of these nucleation-promoting factors. The presence of genes encoding both WASP and SCAR, therefore, provides a molecular correlate for a suite of behaviors that we call "*α*-motility." The conservation and phylogeny of WASP and SCAR indicate that both were present in a common ancestor of living eukaryotes [15,16]. The power of WASP and SCAR as a genomic marker with the ability to identify cryptic pseudopod-forming organisms, together with cell-biology evidence that both WASP and SCAR are required for *α*-motility in well-studied organisms, argues that this widespread behavior arose from single, and ancient origin. Alternatively, it is possible that *α*-motility does not have a single evolutionary origin, but this would require both WASP and SCAR to be co-opted *together* for pseudopod assembly multiple times during eukaryotic history. Because WASP and SCAR are only two of a number of Arp2/3 activators, we have no reason to believe that motility would repeatedly converge on these two in particular.

The fungi represent a large eukaryotic lineage from which the ancestral form of crawling motility has almost completely disappeared. The fungi, together with the metazoans and a handful of protists, form a major clade known as the "opisthokonts" (**Fig 1**). Our identification of *α*-motility in a fungal species argues that the ancestor of all the opisthokonts was capable of fast, pseudopod-associated crawling and that multicellular fungi represent lineages that have lost *α*-motility [50]. This loss appears to coincide with the disappearance from multicellular fungi of cell types lacking a cell wall. We suggest that the limitations on pseudopod formation imposed by a rigid cell wall obviated any possible selection pressure to preserve gene networks specific for fast crawling motility.

Images from earlier studies revealed individual *Bd* zoospores with irregular shapes and "cytoplasmic extensions" [45]. Actin-driven pseudopod formation, however, was not previously described in *Bd* cells, in part because this species was discovered quite recently—in 1999 [45]—and relatively few studies have been devoted to its cell biology. In addition, *Bd* zoospores are quite small (<5 μm) and highly motile so that visualizing their tiny (<1 μm) pseudopods requires physical confinement and high-resolution microscopy. Finally, because pseudopods appear most frequently during a specific stage of the *Bd* life cycle—in zoospores recently released from zoosporangia—synchronization of cell cultures was crucial. These advances not only enabled us to observe *α*-motility, but also revealed *Bd* zoospores rapidly retracting their flagella by coiling the axonemes into the cell body (**Movie S4**).

The *α*-motility of *Bd* fills an important gap in our understanding of the life cycle of this pathogen. As proposed for other chytrid species [44], *Bd* zoospores may use pseudopods during the initial stages of their interaction with a host: either to move across epithelia or crawl between epithelial cells and invade the underlying stroma. Alternatively, our observation that newly hatched zoospores make more pseudopods suggests that *Bd* may rely on *α*-motility to crawl along the epithelial surface to uninfected tissues, or to exit the host.

Imaging chytrid zoospores provided key evidence for the involvement of WASP and SCAR in a conserved mode of cell migration, but further exploration of WASP and SCAR function in *Bd* was hampered by several factors. Firstly, the small size of *Bd* zoospores (<5 μm) poses challenges to live-cell imaging. Secondly, a lack of genetic tools for this species makes it difficult to fluorescently label or deplete proteins in the cells. Thirdly, the lack of potent and specific chemical inhibitors of WASP and SCAR [51,52] means that it is currently impossible to disrupt their activity chemically.

Several protein families are known to stimulate nucleation activity of the Arp2/3 complex, including WASP, SCAR, JMY, and WHAMM. A conventional explanation for this multiplicity of nucleation promoting factors is that these factors direct construction of branched actin networks with different functions at different locations. The conserved connection between WASP, SCAR, and pseudopod formation, however, suggests that this pair of nucleation promoting factors works together to drive the explosive actin polymerization required for pseudopod assembly and fast cell crawling. It is possible that WASP and SCAR act together as a "coincidence detector" that integrates multiple signals and damps formation of spurious pseudopods [53]. This model is supported by studies of the upstream activators of WASP (Cdc42) and SCAR (Rac) [11,12,54,55]. Specifically, Srinivasan et al. suggest that Rac mediates a positive feedback loop required for leading-edge formation, but the stability of the resulting protrusion requires Cdc42 [56].

This model fits the co-localization of WASP and the SCAR regulatory complex at the leading edge (**Fig 2**) and the observation that, while depleting the SCAR regulatory complex leads to a loss of pseudopods in nearly 100% of cells [20], WASP depletion

gives only a partially penetrant phenotype. Although it is possible that this is due to residual WASP protein, this seems an insufficient explanation as WASP knockout mice also show only a partial defect in the gross motility of neutrophils *in vivo* [35]. This implies a requirement for SCAR in mammalian cells, with WASP playing a supporting role. However, the two proteins may play opposite roles in *Dictyostelium discoideum,* the only non-metazoan amoeboid organism in which WASP and SCAR have been studied: Myers et al. [57] reported that high levels of WASP expression are required for cell polarization and chemotaxis*,* and Veltman et al. [19] found that WASP partially compensates for a deletion of SCAR, maintaining cell motility. This coincidence detection model may also explain the rhino cell morphology observed in WASP-depleted cells: if the formation of robust pseudopods requires activation of Arp2/3 by both WASP and SCAR, the resulting more sparsely branched actin networks generated by SCAR-depleted cells might collapse and coalesce into the observed rhino horn structures.

Our results are supported by papers showing that blood cells rely on WASP for efficient cell migration [35,58-65], and others suggesting that WASP plays a direct role in protrusion formation, including pseudopods [24-29]. However, these data have been overshadowed by work in fibroblasts showing that N-WASP is not required for lamellipodia formation, which have been cited as proof that all WASP family proteins are dispensable for motility protrusions in general [66]. Such generalizations depend on two assumptions: that N-WASP and WASP have the same molecular function, and that the assembly of pseudopods and lamellipodia use the same molecular pathways. However, recent molecular replacement studies have shown that WASP and the ubiquitously expressed N-WASP have different functions and cannot compensate for each other [67]. Furthermore, when one considers the large body of mammalian WASP literature in the light of distinct modes of motility, a simple pattern emerges: cells that do not express WASP do not make pseudopods; WASP is only expressed in blood cells, and these cells use WASP for pseudopod-based migration.

Although a large number of eukaryotes make pseudopods (**Fig 1**), only two such lineages are currently molecularly tractable: animals and *Dictyostelium*. Experimental data in both of these lineages confirm that pseudopod formation involves both WASP and SCAR proteins. Taken together, this indicates that while the adhesion-dependent migration used by some animal cell types may require a single Arp2/3 activator (SCAR), the explosive actin polymerization required to build three-dimensional pseudopods involves both SCAR and WASP, and both proteins are conserved together to facilitate this evolutionarily ancient mode of cell motility.

Materials and Methods

Antibodies and Western Blotting: anti-WASP (human) antibody was from Santa Cruz (H-250), as was anti-WAVE2 (C-14), anti-tubulin was from Sigma (DM1A), and anti-actin from Calbiochem (JLA20). Western blotting was conducted using standard protocols and horseradish-peroxidase-conjugated secondary antibodies (Jackson

Laboratories). Florescent secondary antibodies for immunofluorescence were from Molecular Probes (A-11031 and A11029).

Immunofluorescence: HL-60 cells were plated on glass coated with 100 ug/mL bovine plasma fibronectin resuspended in PBS (Sigma, catalog # F4759) for 30 minutes at 37C, fixed for 20 minutes with 4% paraformaldehyde in cytoskeleton buffer (10 mM MES pH 6.1, 138 mM KCl, 3 mM MgCl, 2 mM EGTA, and 0.32 M sucrose), and processed for immunofluorescence using standard protocols. Briefly, cells were permeabilized in PBS-T (PBS supplemented with 0.1% reduced Triton X-100), blocked with 2% BSA in PBS-T, stained for 20 minutes in blocking buffer supplemented with 66 nM florescent phalloidin, followed by antibody and secondary staining in blocking buffer.

Generation of HL-60 cell lines: HL-60 lines were derived from ATCC #CCL-240, and were grown in medium RPMI 1640 supplemented with 15% FBS, 25 mM Hepes, and 2.0g/L NaHCO3, and grown at 37C and 5% CO2. WASP-KD was achieved using Sigma's Mission Control shRNA vector (TRCN0000029819), with corresponding control vector expressing anti-GFP shRNA (Catalog# SHC005). Lentivirus was produced in HEK293T grown in 6-well plates and transfected with equal amounts of the lentiviral backbone vector (either protein expression vector derived from pHRSIN-CSGW [68], or shRNA expression vectors described above), pCMVΔ8.91 (encoding essential packaging genes) and pMD2.G (encoding VSV-G gene to pseudotype virus). After 48hr, the supernatant from each well was removed, centrifuged at 14,000 g for 5 minutes to remove debris and then incubated with ~1x10^6 HL-60 cells suspended in 1 mL complete RPMI for 5-12 hours. Fresh medium was then added and the cells were recovered for 3 days to allow for target protein or shRNA expression. TagRFPt-WASP fusion was cloned by first swapping out eGFP for TagRFP-T [69] in the pHRSIN-CSGW by PCR amplifying TagRFP-T with 5'CCCGGGATCCACCGGTCGCCACCATGGTGTCTAAGGGCGAAGAGCTGATTAAG G3' and 5'GAGTCGCGGCCGCTTTAACTAGTCCCGCTGCCCTTGTACAGCTCGTCCATGCCA TTAAGTTTGTGCCCC3' primers, and cloning the resulting PCR product into pHRSIN-CSGW using NotI and BamHI to produce the pHR-TagRFP-T vector. Then, the WASP open reading frame was PCR amplified from cDNA (NCBI accession BC012738) using 5'GCACTAGTATGAGTGGGGGCCCAATGGGAGGAA3' and 5'AAGCGGCCGCTCAGTCATCCCATTCATCATCTTCATCTTCA3' primers, and cloned into the pHR-TAGRFP-T backbone using NotI and SpeI to result in a single open reading frame containing TagRFPt, a flexible linker (amino acids GSGTS), followed by full length WASP. The WASP shRNA rescue vector was cloned by inserting a P2A cleavage site {Kim:2011*Bd*} between the linker and a WASP open reading frame edited with site-directed mutagenesis to contain three silent mutations within the shRNA-targetting region (5'cgagacctctaaacttatcta3' was changed to 5'CGAaACCTCTAAgCTcATCTA3', with silent mutations in lower case). A corresponding control vector was designed to express TagRFPt with the flexible linker, but no portion of WASP. The Hem1-YFP line was previously described [20]. shRNA lines were selected by puromycin (1ug/mL for at least 1 week), and florescent cell lines

by florescence-activated cell sorting (FACS). HL-60 cells were differentiated by treatment with 1.3% DMSO for 5 days.

Cytometry: FACS analysis was performed on a FACSCalibur analyzer (BD), Data were analyzed with FlowJo software (Tree Star) and dead cells were gated out using forward and side scatter for all analyses. A FACS Aria II was used for sorting. All FACS analysis was performed at the Laboratory for Cell Analysis (UCSF).

Imaging: EZ-TAXIScan (Effector Cell Institute, Tokyo) analysis of HL-60 cell migration between glass surfaces was conducted as previously described [38]. Fixed HL-60 cells were imaged with a 100× 1.40 NA oil Plan Apo objective on a motorized inverted microscope (Nikon Ti-E) equipped with a spinning disk (Yokogawa CSU22) and EMCCD camera (Photometrics Evolve). Live TIRF images were acquired by plating HL-60 cells on coverglass cleaned by 30 minutes incubation in 3M NaOH, followed by four washes with PBS, pH 7.2, coated for 30 minutes with 100ug/mL bovine fibronectin (Sigma F4759) resuspended in PBS. TIRF microscopy images were acquired on a Nikon TE2000 inverted microscope equipped with a 1.45 NA oil 60× or 100× PlanApo TIRF objective and an EMCCD (Andor iXon+), using previously described imaging conditions [33]. Fixed chytrid cells were imaged using an inverted microscope (Nikon Ti-E, Tokyo, Japan) equipped with a spinning-disk confocal system with 33 um pinholes and a 1.8× tube lens (Spectral Diskovery), a Nikon 60× 1.45 NA Apo TIRF objective, and a CMOS camera (Andor Zyla 4.2). DIC microscopy was performed on an inverted microscope (Nikon Ti-E) with a light-emitting diode illuminator (Sutter TLED) and a Nikon 100× 1.45 NA Apo TIRF objective; images were acquired on a CMOS camera (Andor Zyla 4.2). All microscopy hardware was controlled with Micro-Manager software [70]. Image analysis was performed with the ImageJ bundle Fiji.

Quantitation of actin polymerization: HL-60 cells were depolarized in serum free medium supplemented with 2% low-endotoxin BSA (Sigma) for 1 hour at 37C and 5% CO2 before simulation with 20nM fMLP for the indicated time. Cells were immediately fixed with 4% paraformaldehyde in cytoskeleton buffer on ice for 20 minutes, stained with PBS supplemented with 2% BSA, 0.1% triton X-100, and 66 nM Alexaflor-488 conjugated phalloidin (Molecular Probes, catalog # A12379) for 20 minutes, and washed thrice with PBST before FACS analysis.

Transferrin uptake assays: 5×10^6 differentiated HL-60 cells were washed twice with ice-cold serum-free growth medium (SF), transferred to 37C for 5 minutes (to clear surface-bound transferrin), and chilled on ice for 1 minute. An equal volume of cold SF supplemented with 100ug/mL Alexa488 conjugated transferrin (Molecular Probes T-13342) was added, and incubated on ice for 10 minutes. Cells were then washed twice with cold SF medium, transferred to 37C for the indicated time period, washed twice with ice-cold acid buffer (8.76 g NaCl, 9.74 g MES in 900 mL, pH to 4.0, water to 1 L), fixed in 4% paraformaldehyde in 1x PBS for 20 minutes, and washed twice more with ice-cold PBS before immediate FACS analysis.

Amoeboid motility of Chytrid zoospores: *Batrachochytrium dendrobatidis* strain JEL423 was obtained from the laboratory of Joyce Longcore (University of Maine), and were grown in 1% tryptone at 25C. Before imaging, cultures were pseudo-synchronized by three washes in 1% tryptone, and zoospores harvested 2 hours later, passed through a 40um filter (Falcon), and collected by centrifuging at 1,200 g for 5 minutes. Cells were imaged with while sandwiched between a #1.5 glass coverslip and glass slide (cleaned by sonicating in pure water) separated using 5 µm glass microspheres (Bangs Laboratories) while treated with 10 uM CK-666 (Sigma), or DMSO carrier alone. Coverslip and glass slide were sonicated in deionized water, and dried. For visualization of polymerized actin: cells were fixed for 20 minutes in fixation buffer (140 mM KCl, 1 mM $MgCl_2$, 2 mM EGTA, 20 mM Hepes pH7.5, 0.2% BSA, 320 mM sucrose) supplemented with 4% paraformaldehyde while settling onto Poly-L-Lysine coated coverslips, permeabilized with 0.1% triton X-100, incubated for 20 minutes with Alexa488-labeled phalloidin (Invitrogen), rinsed 4 times, and imaged as above.

Acknowledgements:

We would like to thank Jasmine Pare for help with cell culture and cell migration assays, and Joyce Longcore, Jason Stajich, and Erica Rosenblum for strains and helpful discussions. This work was supported by the National Institute of General Medical Sciences of the National Institutes of Health (R01-GM061010 to R.D.M.), by the Howard Hughes Medical Institute Investigator program (R.D.M.), and by a postdoctoral fellowship from the Helen Hay Whitney Foundation supported by the Howard Hughes Medical Institute (L.K.F.-L.).

References:

1. Paluch EK, Raz E. The role and regulation of blebs in cell migration. Curr Opin Cell Biol. 2013;25: 582–590. doi:10.1016/j.ceb.2013.05.005

2. Lämmermann T, Sixt M. Mechanical modes of “amoeboid” cell migration. Curr Opin Cell Biol. 2009;21: 636–644. doi:10.1016/j.ceb.2009.05.003

3. Rodriguez MA, LeClaire LL, Roberts TM. Preparing to move: assembly of the MSP amoeboid motility apparatus during spermiogenesis in Ascaris. Cell Motil Cytoskeleton. 2005;60: 191–199. doi:10.1002/cm.20058

4. Lämmermann T, Bader BL, Monkley SJ, Worbs T, Wedlich-Söldner R, Hirsch K, et al. Rapid leukocyte migration by integrin-independent flowing and squeezing. Nature. 2008;453: 51–55. doi:10.1038/nature06887

5. Bergert M, Chandradoss SD, Desai RA, Paluch E. Cell mechanics control rapid transitions between blebs and lamellipodia during migration. Proc Natl Acad Sci USA. 2012;109: 14434–14439. doi:10.1073/pnas.1207968109

6. Liu Y-J, Le Berre M, Lautenschlaeger F, Maiuri P, Callan-Jones A, Heuzé M, et al. Confinement and low adhesion induce fast amoeboid migration of slow mesenchymal cells. Cell. 2015;160: 659–672. doi:10.1016/j.cell.2015.01.007

7. Petrie RJ, Yamada KM. Fibroblasts Lead the Way: A Unified View of 3D Cell Motility. Trends Cell Biol. 2015;25: 666–674. doi:10.1016/j.tcb.2015.07.013

8. Buenemann M, Levine H, Rappel W-J, Sander LM. The role of cell contraction and adhesion in dictyostelium motility. Biophys J. 2010;99: 50–58. doi:10.1016/j.bpj.2010.03.057

9. Butler KL, Ambravaneswaran V, Agrawal N, Bilodeau M, Toner M, Tompkins RG, et al. Burn injury reduces neutrophil directional migration speed in microfluidic devices. Gelain F, editor. PLoS ONE. Public Library of Science; 2010;5: e11921. doi:10.1371/journal.pone.0011921

10. Winter D, Podtelejnikov AV, Mann M, Li R. The complex containing actin-related proteins Arp2 and Arp3 is required for the motility and integrity of yeast actin patches. Curr Biol. 1997;7: 519–529.

11. Rohatgi R, Ma L, Miki H, Lopez M, Kirchhausen T, Takenawa T, et al. The interaction between N-WASP and the Arp2/3 complex links Cdc42-dependent signals to actin assembly. Cell. 1999;97: 221–231.

12. Koronakis V, Hume PJ, Humphreys D, Liu T, Hørning O, Jensen ON, et al. WAVE regulatory complex activation by cooperating GTPases Arf and Rac1. Proc Natl Acad Sci USA. 2011;108: 14449–14454. doi:10.1073/pnas.1107666108

13. Moreau V, Frischknecht F, Reckmann I, Vincentelli R, Rabut G, Stewart D, et al. A complex of N-WASP and WIP integrates signalling cascades that lead to actin polymerization. Nat Cell Biol. 2000;2: 441–448. doi:10.1038/35017080

14. Zalevsky J, Lempert L, Kranitz H, Mullins RD. Different WASP family proteins stimulate different Arp2/3 complex-dependent actin-nucleating activities. Curr Biol. 2001;11: 1903–1913.

15. Veltman DM, Insall RH. WASP family proteins: their evolution and its physiological implications. Mol Biol Cell. 2010; 21: 2880–2893.

16. Kollmar M, Lbik D, Enge S. Evolution of the eukaryotic ARP2/3 activators of the WASP family: WASP, WAVE, WASH, and WHAMM, and the proposed new family members WAWH and …. BMC research notes. 2012; 5: 88.

17. Steffen A, Rottner K, Ehinger J, Innocenti M, Scita G, Wehland J, et al. Sra-1 and Nap1 link Rac to actin assembly driving lamellipodia formation. EMBO J. 2004;23: 749–759. doi:10.1038/sj.emboj.7600084

18. Miki H, Suetsugu S, Takenawa T. WAVE, a novel WASP-family protein involved in actin reorganization induced by Rac. EMBO J. 1998;17: 6932–6941. doi:10.1093/emboj/17.23.6932

19. Veltman DM, King JS, Machesky LM, Insall RH. SCAR knockouts in Dictyostelium: WASP assumes SCAR's position and upstream regulators in pseudopods. J Cell Biol. 2012;198: 501–508. doi:10.1083/jcb.201205058

20. Weiner OD, Rentel MC, Ott A, Brown GE, Jedrychowski M, Yaffe MB, et al. Hem-1 complexes are essential for Rac activation, actin polymerization, and myosin regulation during neutrophil chemotaxis. PLoS Biol. 2006;4: e38. doi:10.1371/journal.pbio.0040038

21. Snapper SB, Takeshima F, Antón I, Liu CH, Thomas SM, Nguyen D, et al. N-WASP deficiency reveals distinct pathways for cell surface projections and microbial actin-based motility. Nat Cell Biol. 2001;3: 897–904. doi:10.1038/ncb1001-897

22. Lommel S, Benesch S, Rottner K, Franz T, Wehland J, Kühn R. Actin pedestal formation by enteropathogenic Escherichia coli and intracellular motility of Shigella flexneri are abolished in N-WASP-defective cells. EMBO Rep. 2001;2: 850–857. doi:10.1093/embo-reports/kve197

23. Sarmiento C, Wang W, Dovas A, Yamaguchi H, Sidani M, El-Sibai M, et al. WASP family members and formin proteins coordinate regulation of cell protrusions in carcinoma cells. The Journal of Cell Biology. 2008;180: 1245–1260. doi:10.1083/jcb.200708123

24. Jones GE, Zicha D, Dunn GA, Blundell M, Thrasher A. Restoration of podosomes and chemotaxis in Wiskott-Aldrich syndrome macrophages following induced expression of WASp. Int J Biochem Cell Biol. 2002;34: 806–815.

25. Burns S, Thrasher AJ, Blundell MP, Machesky L, Jones GE. Configuration of human dendritic cell cytoskeleton by Rho GTPases, the WAS protein, and differentiation. Blood. 2001;98: 1142–1149.

26. Badolato R, Sozzani S, Malacarne F, Bresciani S, Fiorini M, Borsatti A, et al. Monocytes from Wiskott-Aldrich patients display reduced chemotaxis and lack of cell polarization in response to monocyte chemoattractant protein-1 and formyl-methionyl-leucyl-

phenylalanine. J Immunol. 1998;161: 1026–1033.

27. Jones RA, Feng Y, Worth AJ, Thrasher AJ, Burns SO, Martin P. Modelling of human Wiskott-Aldrich syndrome protein mutants in zebrafish larvae using in vivo live imaging. J Cell Sci. 2013;126: 4077–4084. doi:10.1242/jcs.128728

28. Shi Y, Dong B, Miliotis H, Liu J, Alberts AS, Zhang J, et al. Src kinase Hck association with the WASp and mDia1 cytoskeletal regulators promotes chemoattractant-induced Hck membrane targeting and activation in neutrophils. Biochem Cell Biol. 2009;87: 207–216. doi:10.1139/O08-130

29. Ishihara D, Dovas A, Park H, Isaac BM, Cox D. The chemotactic defect in wiskott-Aldrich syndrome macrophages is due to the reduced persistence of directional protrusions. PLoS ONE. Public Library of Science; 2012;7: e30033. doi:10.1371/journal.pone.0030033

30. Maugis B, Brugués J, Nassoy P, Guillen N, Sens P, Amblard F. Dynamic instability of the intracellular pressure drives bleb-based motility. J Cell Sci. 2010;123: 3884–3892. doi:10.1242/jcs.065672

31. Collins SJ, Gallo RC, Gallagher RE. Continuous growth and differentiation of human myeloid leukaemic cells in suspension culture. Nature. 1977;270: 347–349.

32. Collins SJ, Ruscetti FW, Gallagher RE, Gallo RC. Terminal differentiation of human promyelocytic leukemia cells induced by dimethyl sulfoxide and other polar compounds. Proc Natl Acad Sci USA. 1978;75: 2458–2462.

33. Weiner OD, Marganski WA, Wu LF, Altschuler SJ, Kirschner MW. An actin-based wave generator organizes cell motility. PLoS Biol. 2007;5: e221. doi:10.1371/journal.pbio.0050221

34. Axelrod D. Cell-substrate contacts illuminated by total internal reflection fluorescence. J Cell Biol. 1981;89: 141–145.

35. Snapper SB, Meelu P, Nguyen D, Stockton BM, Bozza P, Alt FW, et al. WASP deficiency leads to global defects of directed leukocyte migration in vitro and in vivo. J Leukoc Biol. 2005;77: 993–998. doi:10.1189/jlb.0804444

36. Burkel BM, Dassow von G, Bement WM. Versatile fluorescent probes for actin filaments based on the actin-binding domain of utrophin. Cell Motil Cytoskeleton. 2007;64: 822–832. doi:10.1002/cm.20226

37. Tilney LG, Hatano S, Ishikawa H, Mooseker MS. The polymerization of actin: its role in the generation of the acrosomal process of certain echinoderm sperm. J Cell Biol. 1973;59: 109–126.

38. Millius A, Weiner OD. Manipulation of neutrophil-like HL-60 cells for the study of directed cell migration. Methods Mol Biol. 2010;591: 147–158. doi:10.1007/978-1-60761-404-3_9

39. Benesch S, Polo S, Lai FPL, Anderson KI, Stradal TEB, Wehland J, et al. N-WASP deficiency impairs EGF internalization and actin assembly at clathrin-coated pits. J Cell

Sci. 2005;118: 3103–3115. doi:10.1242/jcs.02444

40. Merrifield CJ, Qualmann B, Kessels MM, Almers W. Neural Wiskott Aldrich Syndrome Protein (N-WASP) and the Arp2/3 complex are recruited to sites of clathrin-mediated endocytosis in cultured fibroblasts. Eur J Cell Biol. 2004;83: 13–18. doi:10.1078/0171-9335-00356

41. Naqvi SN, Zahn R, Mitchell DA, Stevenson BJ, Munn AL. The WASp homologue Las17p functions with the WIP homologue End5p/verprolin and is essential for endocytosis in yeast. Curr Biol. 1998;8: 959–962.

42. McGraw TE, Subtil A. Endocytosis: biochemical analyses. Curr Protoc Cell Biol. 2001;Chapter 15: Unit 15.3. doi:10.1002/0471143030.cb1503s03

43. Deacon JW. Fungal Biology. Wiley-Blackwell; 2005.

44. Gleason FH, Lilje O. Structure and function of fungal zoospores: ecological implications. Fungal Ecol. 2009;2: 53–59. doi:10.1016/j.funeco.2008.12.002

45. Longcore JE, Pessier AP, Nichols DK. Batrachochytrium Dendrobatidis gen. et sp. nov., a Chytrid Pathogenic to Amphibians. Mycologia. 1999;91: 219–227. doi:10.2307/3761366

46. Berger L, Hyatt AD, Speare R, Longcore JE. Life cycle stages of the amphibian chytrid Batrachochytrium dendrobatidis. Dis Aquat Organ. 2005;68: 51–63. doi:10.3354/dao068051

47. Chodniewicz D, Zhelev DV. Chemoattractant receptor-stimulated F-actin polymerization in the human neutrophil is signaled by 2 distinct pathways. Blood. 2003;101: 1181–1184. doi:10.1182/blood-2002-05-1435

48. Zhelev DV, Alteraifi AM, Chodniewicz D. Controlled pseudopod extension of human neutrophils stimulated with different chemoattractants. Biophys J. 2004;87: 688–695. doi:10.1529/biophysj.103.036699

49. Nolen BJ, Tomasevic N, Russell A, Pierce DW, Jia Z, McCormick CD, et al. Characterization of two classes of small molecule inhibitors of Arp2/3 complex. Nature. 2009;460: 1031–1034. doi:10.1038/nature08231

50. Fritz-Laylin LK, Prochnik SE, Ginger ML, Dacks JB, Carpenter ML, Field MC, et al. The genome of Naegleria gruberi illuminates early eukaryotic versatility. Cell. 2010;140: 631–642. doi:10.1016/j.cell.2010.01.032

51. Bompard G, Rabeharivelo G, Morin N. Inhibition of cytokinesis by wiskostatin does not rely on N-WASP/Arp2/3 complex pathway. BMC Cell Biol. 2008;9: 42. doi:10.1186/1471-2121-9-42

52. Guerriero CJ, Weisz OA. N-WASP inhibitor wiskostatin nonselectively perturbs membrane transport by decreasing cellular ATP levels. Am J Physiol, Cell Physiol. 2007;292: C1562–6. doi:10.1152/ajpcell.00426.2006

53. Stradal TEB, Scita G. Protein complexes regulating Arp2/3-mediated actin assembly.

Curr Opin Cell Biol. 2006;18: 4–10. doi:10.1016/j.ceb.2005.12.003

54. Lebensohn AM, Kirschner MW. Activation of the WAVE complex by coincident signals controls actin assembly. Mol Cell. 2009;36: 512–524. doi:10.1016/j.molcel.2009.10.024

55. Rohatgi R, Ho HY, Kirschner MW. Mechanism of N-WASP activation by CDC42 and phosphatidylinositol 4, 5-bisphosphate. J Cell Biol. 2000;150: 1299–1310.

56. Srinivasan S, Wang F, Glavas S, Ott A, Hofmann F, Aktories K, et al. Rac and Cdc42 play distinct roles in regulating PI(3,4,5)P3 and polarity during neutrophil chemotaxis. J Cell Biol. 2003;160: 375–385. doi:10.1083/jcb.200208179

57. Myers SA, Han JW, Lee Y, Firtel RA, Chung CY. A Dictyostelium homologue of WASP is required for polarized F-actin assembly during chemotaxis. Mol Biol Cell. 2005;16: 2191–2206. doi:10.1091/mbc.E04-09-0844

58. Kumar S, Xu J, Perkins C, Guo F, Snapper S, Finkelman FD, et al. Cdc42 regulates neutrophil migration via crosstalk between WASp, CD11b, and microtubules. Blood. 2012;120: 3563–3574. doi:10.1182/blood-2012-04-426981

59. Anderson SI, Behrendt B, Machesky LM, Insall RH, Nash GB. Linked regulation of motility and integrin function in activated migrating neutrophils revealed by interference in remodelling of the cytoskeleton. Cell Motil Cytoskeleton. 2003;54: 135–146. doi:10.1002/cm.10091

60. Blundell MP, Bouma G, Calle Y, Jones GE, Kinnon C, Thrasher AJ. Improvement of migratory defects in a murine model of Wiskott-Aldrich syndrome gene therapy. Mol Ther. 2008;16: 836–844. doi:10.1038/mt.2008.43

61. Zhang H, Schaff UY, Green CE, Chen H, Sarantos MR, Hu Y, et al. Impaired integrin-dependent function in Wiskott-Aldrich syndrome protein-deficient murine and human neutrophils. Immunity. 2006;25: 285–295. doi:10.1016/j.immuni.2006.06.014

62. Zicha D, Allen WE, Brickell PM, Kinnon C, Dunn GA, Jones GE, et al. Chemotaxis of macrophages is abolished in the Wiskott-Aldrich syndrome. Br J Haematol. 1998;101: 659–665.

63. Dovas A, Gevrey J-C, Grossi A, Park H, Abou-Kheir W, Cox D. Regulation of podosome dynamics by WASp phosphorylation: implication in matrix degradation and chemotaxis in macrophages. J Cell Sci. 2009;122: 3873–3882. doi:10.1242/jcs.051755

64. Worth AJJ, Metelo J, Bouma G, Moulding D, Fritzsche M, Vernay B, et al. Disease-associated missense mutations in the EVH1 domain disrupt intrinsic WASp function causing dysregulated actin dynamics and impaired dendritic cell migration. Blood. 2013;121: 72–84. doi:10.1182/blood-2012-01-403857

65. Binks M, Jones GE, Brickell PM, Kinnon C, Katz DR, Thrasher AJ. Intrinsic dendritic cell abnormalities in Wiskott-Aldrich syndrome. Eur J Immunol. 1998;28: 3259–3267.

66. Small JV, Rottner K. Elementary Cellular Processes Driven by Actin Assembly: Lamellipodia and Filopodia. Actin-based Motility. Dordrecht: Springer Netherlands; 2010.

pp. 3–33. doi:10.1007/978-90-481-9301-1_1

67. Jain N, Thanabalu T. Molecular difference between WASP and N-WASP critical for chemotaxis of T-cells towards SDF-1α. Sci Rep. 2015;5: 15031. doi:10.1038/srep15031

68. Demaison C, Parsley K, Brouns G, Scherr M, Battmer K, Kinnon C, et al. High-level transduction and gene expression in hematopoietic repopulating cells using a human immunodeficiency [correction of imunodeficiency] virus type 1-based lentiviral vector containing an internal spleen focus forming virus promoter. Hum Gene Ther. 2002;13: 803–813. doi:10.1089/10430340252898984

69. Shaner NC, Lin MZ, McKeown MR, Steinbach PA, Hazelwood KL, Davidson MW, et al. Improving the photostability of bright monomeric orange and red fluorescent proteins. Nat Methods. 2008;5: 545–551. doi:10.1038/nmeth.1209

70. Edelstein A, Amodaj N, Hoover K, Vale R, Stuurman N. Computer control of microscopes using μManager. Curr Protoc Mol Biol. 2010;Chapter 14: Unit14.20. doi:10.1002/0471142727.mb1420s92

Figure 1. Only organisms that make pseudopods retain both WASP and SCAR genes.

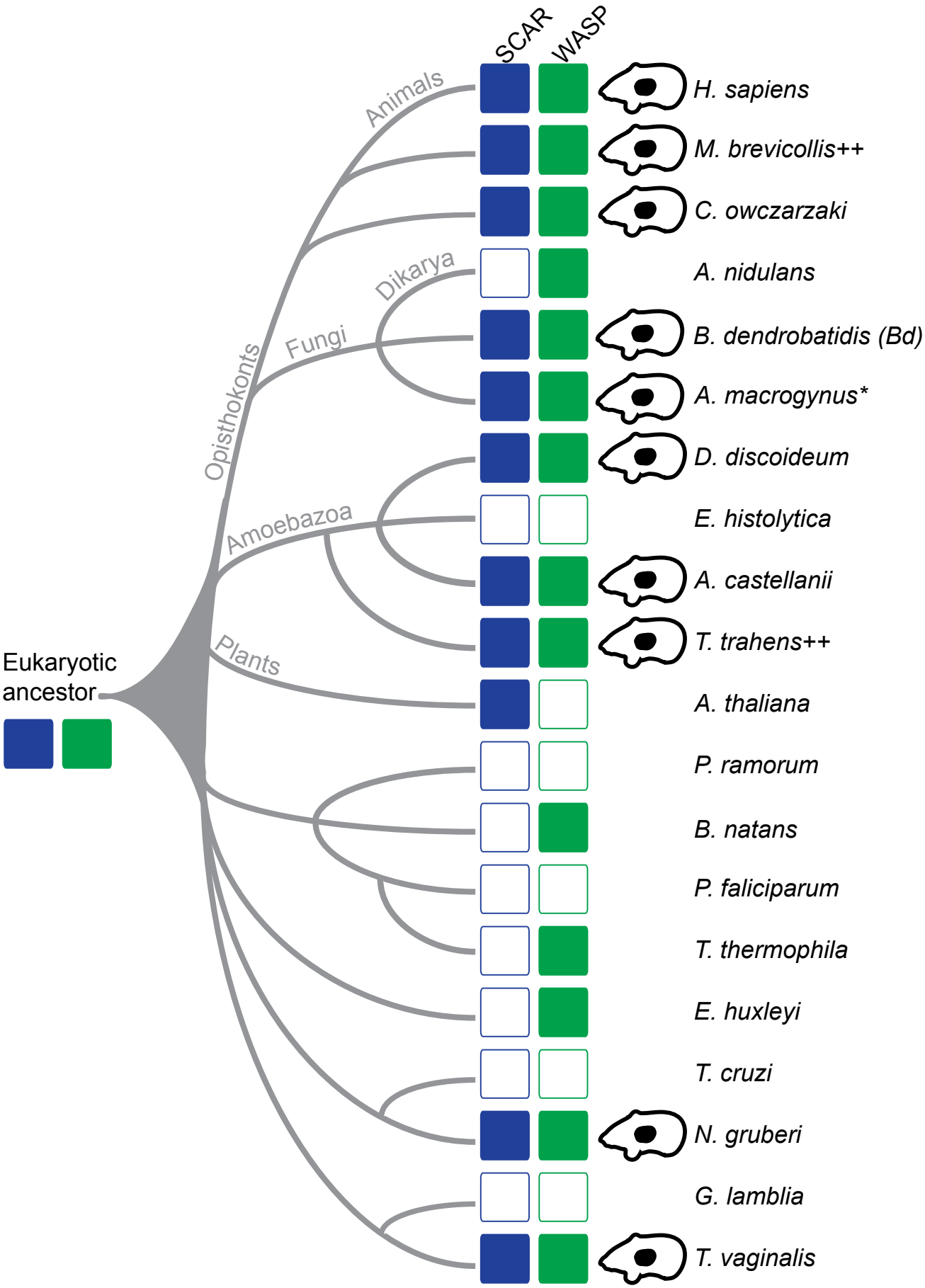

Fig 1. Only organisms that make pseudopods retain both WASP and SCAR genes. Diagram showing the relationships of extant eukaryotes (based on [50]), with presence or absence of SCAR (blue) and WASP (green) genes from complete genome sequences as described [16]. The representative organism whose genome was used for the analysis is listed to the right. For groups with similar morphological and sequence patterns, a single species is used. For example, there is no known plant species that forms pseudopods or retains the WASP gene, so only a single species is shown (*Arabidopsis thaliana*); similarly, *Aspergillus nidulans* represents all dikarya. See [16] for additional sequence information. An amoeba glyph indicates organisms that build pseudopods. Outlined rectangles indicate a lack of identifiable gene. See **Table S1** for citations and full species names. *Although we were not able to find a reference to pseudopod formation in *A. macrogynus*, a relative (*Catenaria anguillulae)* does assemble pseudopods used for motility [44]. Because of this, and the conservation of both WASP and SCAR in *B. dendrobatidis*, we predict this species is also capable of pseudopod formation. ++These species form pseudopods for feeding, rather than motility.

Figure 2: WASP co-localizes with the SCAR complex at the leading edge of neutrophils.

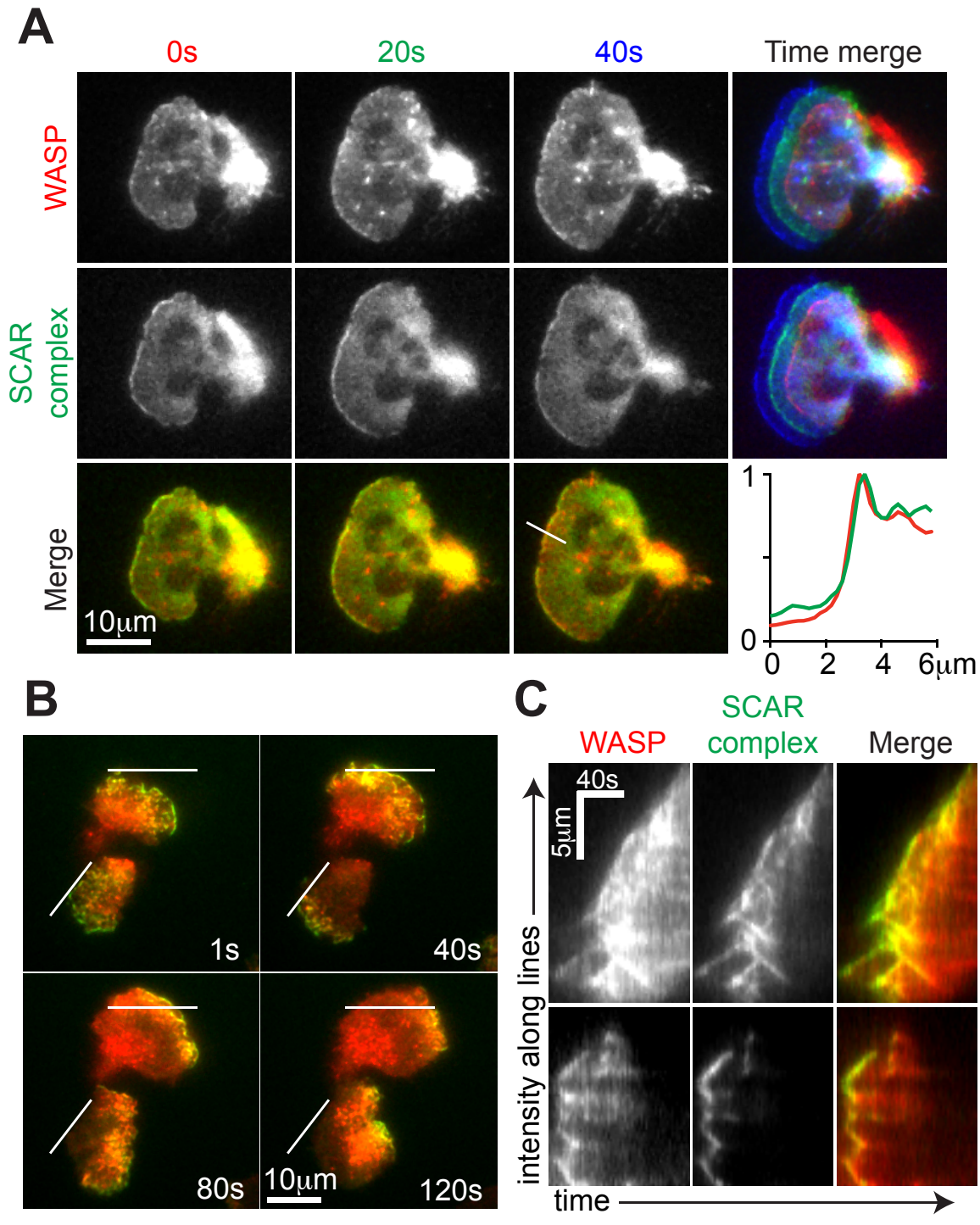

Fig 2: WASP co-localizes with the SCAR complex at the leading edge of neutrophils.

TIRF microscopy of live HL-60 cells expressing TagRFP-WASP and Hem-1-YFP (a component of the SCAR regulatory complex). **(A)** Top: WASP localization in three sequential time points, overlayed on the far right (0 seconds in red, 20 seconds in green, and 40 seconds in blue). Middle: same sequence of images, but for Hem-1. Bottom: overlay of WASP and Hem-1 at each time point. The plot shows line scans of normalized fluorescence intensity of WASP (red) and Hem-1 (green). The location for generating the line scans is shown in the adjacent image. **(B)** Time points from which kymographs in C were generated. Lines correspond to kymographs (top and bottom). **(C)** Kymographs of pseudopods in panel B, showing colocalization of TagRFP-WASP and Hem-1-YFP. See also **Movie S1**.

Figure 3. WASP is crucial for explosive actin polymerization, pseudopod formation, and cell motility of neutrophils.

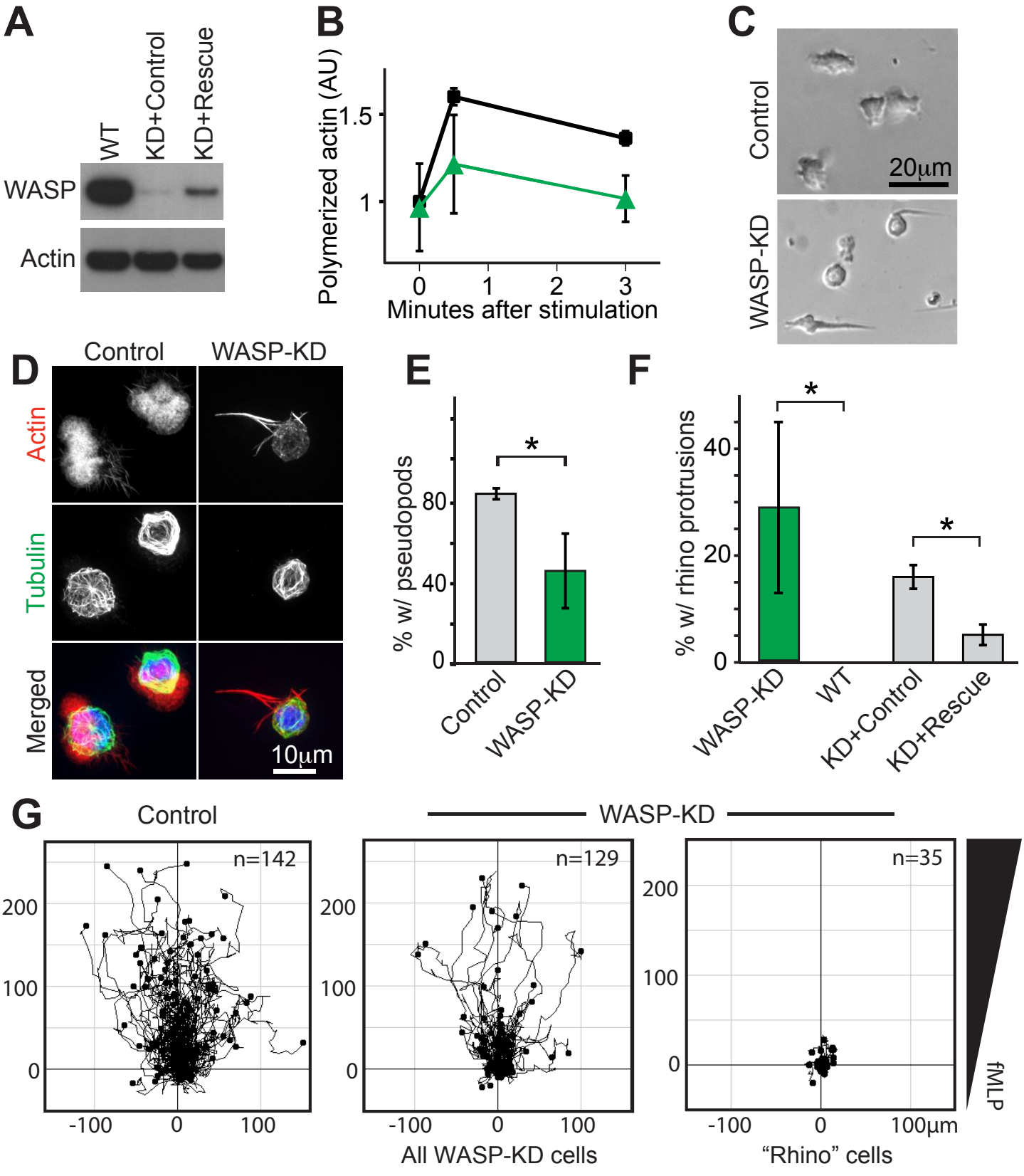

Fig 3. WASP is crucial for explosive actin polymerization, pseudopod formation, and cell motility of neutrophils. (A) Western blots showing WASP expression in control HL-60 cells (WT, left), cells expressing shRNA to WASP and exogenous WASP with three silent mutations in the region corresponding to the shRNA (KD+rescue, right), or cells expressing anti-WASP shRNA and empty vector rescue control (KD+control, middle). Equal amounts of total protein were loaded in each lane, confirmed using actin as a loading control. **(B)** Polymerized actin of control (black squares) and WASP-KD HL-60 cells (green triangles) after stimulation for the indicated time with chemoattractant (20 nM fMLP), stained with florescent phalloidin, and quantified with FACS. 10,000 cells were counted for each sample, and normalized to time zero for control within each experiment. **(C)** Brightfield microscopy of control and WASP knockdown cells. **(D)** Immunofluorescence of control and WASP-KD HL-60 cells showing microtubules (green, antibody-stained), polymerized actin (red, phalloidin-stained), and DNA (blue, DAPI). Note the signature rhino phenotype in the WASP-KD cell. See also **Fig S2**. **(E)** Knockdown of WASP using shRNA reduces the percent of cells that have pseudopods. **(F)** Rescue of rhino protrusion phenotype by expression of shRNA insensitive WASP as described in A. Note: no wildtype cells were observed to exhibit the rhino phenotype. For E-F, bars represent averages and standard deviation from 3 replicates; *p=0.003 using two-tailed paired t-test. **(G)** Worm plots showing the tracks of cell migrating up a chemoattractant gradient: control cells (left), all WASP-KD cells (middle), and only the WASP-KD cells that exhibit the rhino phenotype (right). Cells were imaged 20 minutes, and migration paths overlaid, with time zero at (0,0). The endpoint of each cell's path is shown with a black dot. The number of cells recorded is labeled in each plot. See also **Movie S2.**

Figure 4. Genomic retention of both WASP and SCAR correctly predicts α-motility in the infectious chytrid fungus B. dendrobatidis.

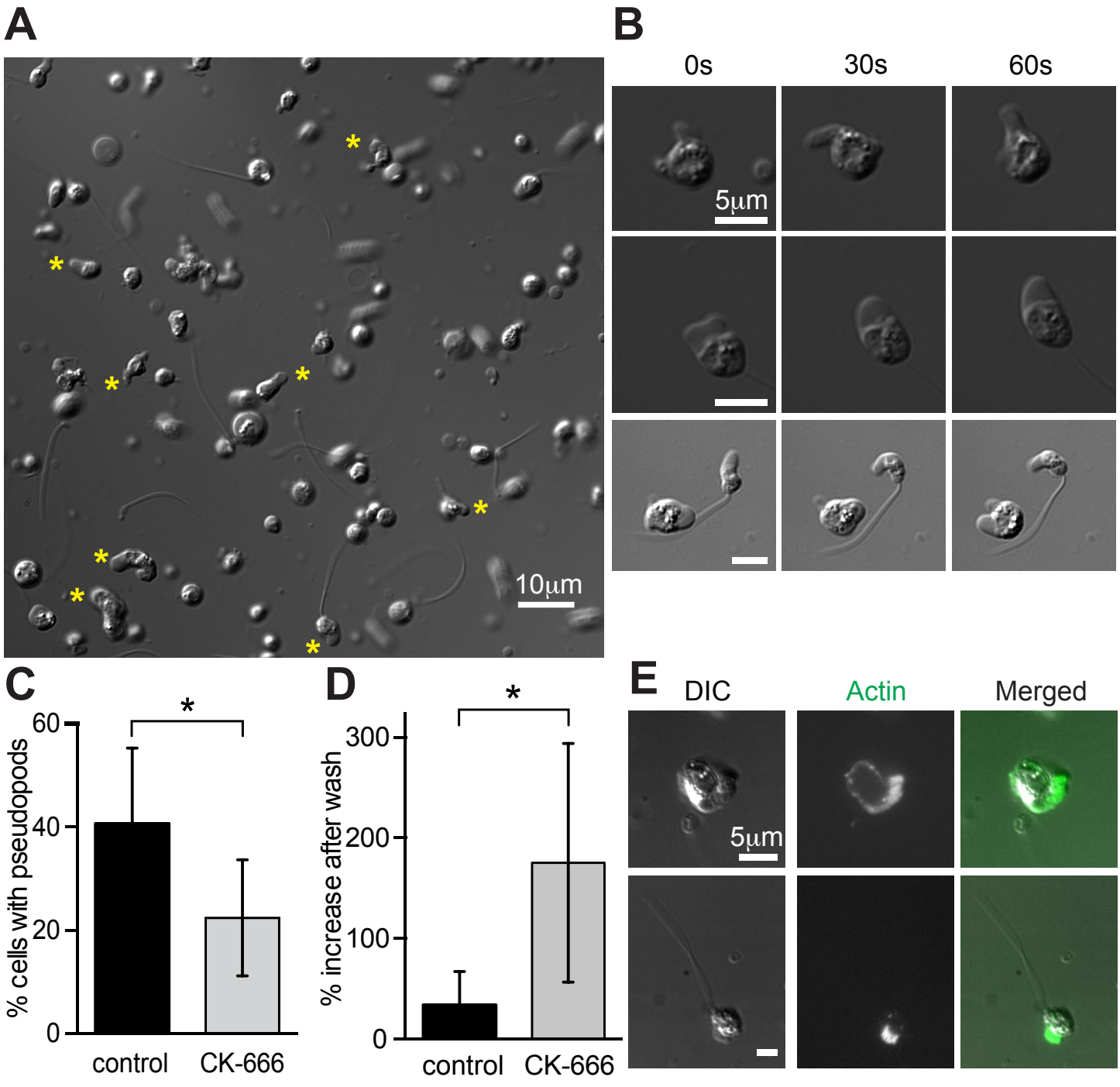

Fig 4. Genomic retention of both WASP and SCAR correctly predicts *α*-motility in the infectious chytrid fungus *B. dendrobatidis*.
(A) DIC image of representative field of pseudo-synchronized *Bd* zoospores. Asterisks are highlighted by cells with obvious pseudopods. Rapidly-swimming flagellate cells are blurred. **(B)** Time lapse showing examples of pseudopods from cells without (top) and with flagella (middle), or one cell of each (bottom). See also **Movie S3**. **(C)** Fewer zoospores make pseudopods when treated with CK-666, an inhibitor of Arp2/3 activity. **(D)** Inhibition by CK-666 is reversible: the percentage of cells that exhibit pseudopods increases after washing CK-666 out of the media. For C-D, bars represent averages and standard deviation from 4 replicates, and each individual replicate exhibited the same trend as the average; *p=0.03 using one-tailed paired t-test. **(E)** Fixed cells with a flagellum (bottom) and without (top) stained with fluorescent phalloidin reveal a thin shell of cortical actin surrounding the cell body and a dense network of filamentous actin filling the pseudopods.